Manufacture of a combined primary and tertiary mirror for the Large Synoptic Survey Telescope

H. M. Martin[a], J. H. Burge[a,b], B. Cuerden[a], W. B. Davison[a], J. S. Kingsley[a], R. D. Lutz[a], S. M. Miller[a], M. Tuell[a]

[a]Steward Observatory, University of Arizona, Tucson, AZ 85721, USA
[b]College of Optical Sciences, University of Arizona, Tucson, AZ 85721, USA

ABSTRACT

The Large Synoptic Survey Telescope uses a unique optomechanical design that places the primary and tertiary mirrors on a single glass substrate. The honeycomb sandwich mirror blank was formed in March 2008 by spin-casting. The surface is currently a paraboloid with a 9.9 m focal length matching the primary. The deeper curve of the tertiary mirror will be produced when the surfaces are generated. Both mirrors will be lapped and polished using stressed laps and other tools on an 8.4 m polishing machine. The highly aspheric primary mirror will be measured through a refractive null lens, and a computer-generated hologram will be used to validate the null lens. The tertiary mirror will be measured through a diffractive null corrector, also validated with a separate hologram. The holograms for the two tests provide alignment references that will be used to make the axes of the two surfaces coincide.

Keywords: telescopes, optical fabrication, optical testing, aspheres, active optics

1. INTRODUCTION

The Large Synoptic Survey Telescope (LSST) uses three mirrors to provide a 3.5-degree field of view.[1] This powerful optical design is coupled with a unique *physical* design that places the annular 8.4 m primary mirror (M1) and 5.1 m tertiary mirror (M3) on the surface of a single glass substrate. This design allows the alignment of M1 and M3 to be controlled at the time of manufacture, eliminating the need for active control of the associated degrees of freedom in the telescope. It also improves the stiffness of the annular primary. The optical layout is shown in Figure 1.

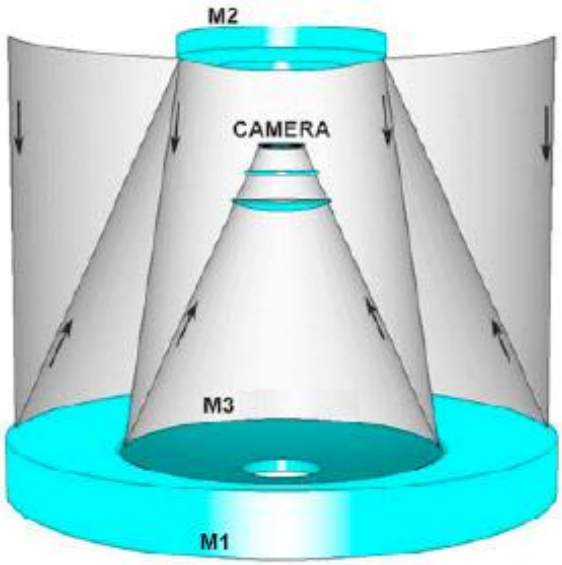

Figure 1. Optical layout of the LSST, showing the 8.4 m primary (M1), 3.4 m convex secondary (M2), 5.1 m tertiary (M3), refractive field corrector, and detector.

Advanced Optical and Mechanical Technologies in Telescopes and Instrumentation, edited by Eli Atad-Ettedgui, Dietrich Lemke, Proc. of SPIE Vol. 7018, 70180G, (2008) · 0277-786X/08/$18 · doi: 10.1117/12.789959

The combined mirror is a honeycomb sandwich and is being made at the Steward Observatory Mirror Lab. The honeycomb sandwich has a high ratio of stiffness to weight and a low thermal time constant with its thin glass sections and ventilation of the internal surfaces. It promises to give excellent performance. While the combined mirror simplifies telescope operation by removing several degrees of freedom from the active alignment, it also makes it essential that we get the alignment right during manufacture. We are providing a redundant pair of alignment measurements, both of which have the accuracy required to demonstrate alignment within the tolerances.

The remainder of this paper presents the design, manufacturing plan and status of the combined mirror. Section 2 presents the requirements for fabrication. Section 3 describes the physical design. Section 4 gives an overview of the manufacturing plan, while Sections 5 and 6 describe the casting, generating and polishing in more detail. Section 7 outlines the plan for measurements. Section 8 summarizes the paper.

2. REQUIREMENTS

2.1 Optical design

Some of the optical parameters of the LSST M1 and M3 are listed in Table 1 along with tolerances. The radii listed are for the laboratory temperature of 21°C and take account of the expansion coefficient of the Ohara E6 borosilicate glass (2.8 ppm/K) and the mean operational temperature of 11.5°C. M1 is an 8.4 m f/1.18 hyperboloid while M3 is a 5.1 m f/0.82 oblate ellipsoid. Both mirror surfaces contain additional aspheric terms. The two surfaces intersect at a radius of 2.533 m. An annulus 50 mm wide, centered on the intersection radius, is excluded from the clear aperture over which an accurate figure must be maintained.

Table 1. Optical design parameters for the LSST mirrors

parameter	M1	M3
outer clear aperture diameter	8360 mm	5016 mm
inner clear aperture diameter	5116 mm	1100 mm
vertex height (relative to rear surface)	473.6 mm	239.8 mm
radius of curvature	19835.5 ± 1 mm	8344.7 ± 1 mm
conic constant	-1.2150 ± 0.0002	0.1550 ± 0.0001

2.2 Figure accuracy

The figure accuracies of the two surfaces are specified in terms of the wavefront structure function, which gives the allowed error as a function of spatial scale. The structure function is the mean square wavefront difference between points in the aperture as a function of their separation. The specifications have the form of the standard structure function for seeing (for short-exposure images). There is an additional allowance for an insignificant scattering loss due to small-scale structure. Figure 2 shows the allowed errors.

2.3 Active optics and figure accuracy

The glass substrate with both optical surfaces will be held in the telescope by an active support system containing 156 actuators distributed over the rear surface of the mirror. The structure function specifications apply to the mirror figures after correction of low-order bending modes (large-scale errors) that are easily corrected with the active support. Astigmatism is the prime example of a large-scale error that is easily corrected. Several hundred nm of astigmatism can be corrected with forces of several N, and can therefore be ignored in the fabrication process.

This assumption of active correction is standard procedure in the manufacture of large mirrors. A simulated correction based on calculated mirror bending is generally used to determine which errors can be ignored. The simulated correction can be applied to constant errors, or to errors that vary from measurement to measurement due to small changes in support forces or temperature gradients. For flexible bending modes like astigmatism, variations from day to day can be significant, but they can be ignored as long as the magnitude is within the correctable range. The same thing happens in the telescope, where the errors are measured with a wavefront sensor and corrected with the active supports.

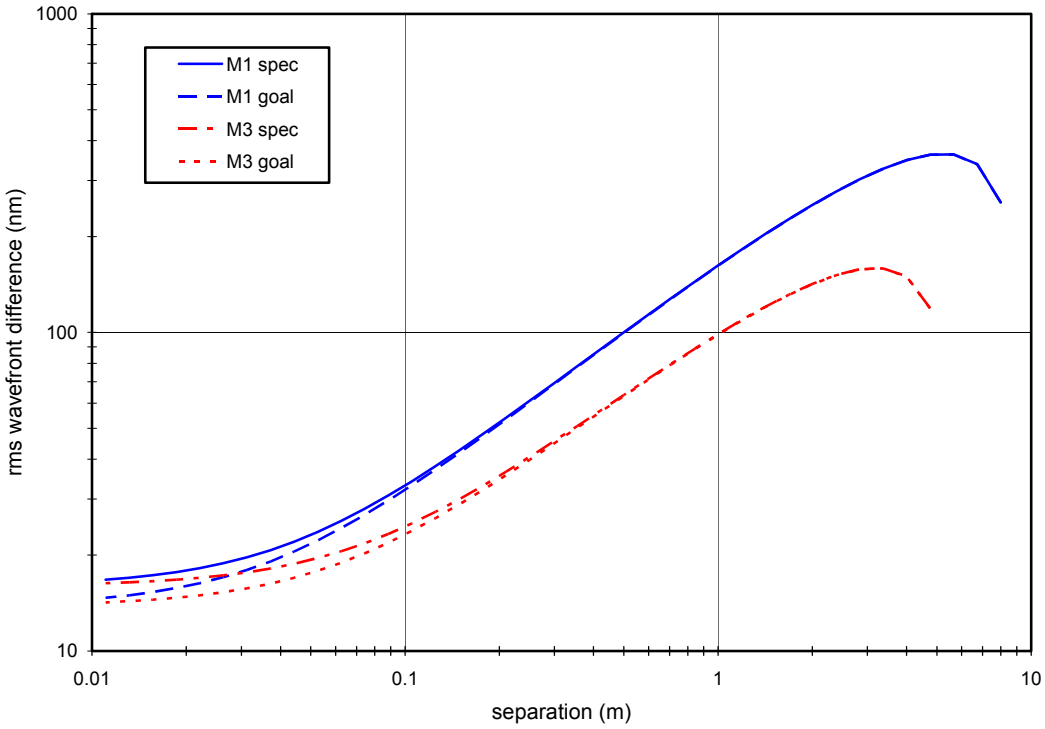

Figure 2. Specification for figure errors on both mirrors. The quantity plotted is the rms wavefront difference as a function of separation, equal to the square root of the wavefront structure function.

For LSST, this procedure is complicated by the fact that both M1 and M3 optical surfaces are on the same piece of glass and respond to the same actuator forces. Any bending of the substrate to correct the M1 optical shape will also change the shape of M3. This common bending is no problem in the telescope—assuming the combined mirror is made with acceptably small low-order shape errors to begin with—because the combined effect of M1 and M3 can be measured with a wavefront sensor and the substrate shape can be optimized. It does, however, present a potential problem for manufacturing, because it would be possible to figure each mirror surface separately so its low-order errors can be corrected by bending, when in fact the bending modes of the combined mirror do not allow correction of both surfaces simultaneously. This manufacturing issue can be resolved by measuring both surfaces simultaneously in the lab and figuring them so that any low-order aberrations can be corrected simultaneously. We have designed the LSST test systems to allow simultaneous measurements.

We have also performed a direct simulation of active correction and shown that any realistic low-order errors on the mirror surfaces, even if they are not controlled by simultaneous measurements in the lab, can be corrected in the telescope. These errors are correctable because (a) low-order bending affects the M1 surface more than the M3 surface, and (b) the bending modes of the combined substrate tend to put similar shapes (although different magnitudes) of errors on the two mirror surfaces. Reason (a) means one can correct a large fraction of the error by ignoring M3, and reason (b) means the net wavefront error tends to have a shape that can be corrected by bending the substrate. For example, astigmatism with different magnitudes and rotation angles on the three mirrors will produce a wavefront with some net astigmatism, which can be corrected by bending the substrate astigmatically with a magnitude and rotation angle that cancels the wavefront error. The net result, as demonstrated by the simulations, is that small amounts of independent low-order shape errors in M1 and M3 can be reduced to negligible wavefront errors by bending the substrate with active optics.

While the simulations are reassuring, we can achieve even higher confidence in the system performance by measuring the two surfaces simultaneously, or at least while the combined mirror has a constant shape. The lab tests will provide the capability to measure the two surfaces simultaneously. The test optics for M3 are deployable. Their support structure will obscure part of M1's measurement when they are deployed, but this obscuration will have little impact on the measurement of large-scale errors, and only large-scale errors require simultaneous measurements. To obtain the

most accurate, unobscured measurements of both surfaces, we will measure M1, then M3, then M1 again over a period of about an hour. This procedure will detect any drift in the shape of the substrate, and will eliminate first-order drift when the two measurements of M1 are averaged. We plan to demonstrate that this "sandwich" set of measurements is equivalent to simultaneous measurement. With simultaneous measurements of the two surfaces, we can figure one or both surfaces so they have consistent low-order aberrations, i. e. aberrations that can be corrected with a single set of acceptably small forces applied to the substrate.

2.4 Alignment of the two mirrors

A large part of the reason for combining the two mirrors is to fix their relative alignment during manufacture, eliminating the need to control it actively in the telescope. The degrees of freedom that must be controlled are spacing, tilt and lateral displacement of the optical axis. Lateral displacement of the optical axis is defined as a pivot of the mirror surface around its center of curvature, making this degree of freedom orthogonal to tilt of the surface. Table 2 lists the tolerances. One set of tolerances applies to the alignment of M1 relative to the mirror blank, whose axis is defined by the flat rear surface and the outer diameter. A second set applies to the alignment of M3 relative to M1. The displacement listed is the lateral separation of the two axes at the primary mirror surface.

Table 2. Tolerances for alignment of the two mirrors

parameter	M1 relative to mirror blank	M3 relative to M1
axial spacing	±2 mm	±2 mm
tilt	30 arcseconds	4 arcseconds
lateral displacement of optical axis	1 mm	1 mm

3. PHYSICAL DESIGN OF THE MIRRORS

The combined mirror is a single piece of glass with the M1 surface covering the outer annulus 2.5 m < r < 4.2 m, and M3 covering the inner annulus 0.5 m < r < 2.5 m. The blank is a honeycomb sandwich shown in Figure 3. It has a continuous flat back plate 25 mm thick, and a uniform facesheet 28 mm thick. The uniform facesheet is achieved by machining the two curves into the ceramic fiber mold that forms the honeycomb sandwich. The facesheet and back plate are connected by ribs, 12 mm thick, in a hexagonal pattern with a center-center spacing of 192 mm. In order to maintain roughly equal rib spacing near the edge of the mirror, the pattern makes a gradual transition to a ring of identical pentagons. Apart from the size of the center hole, the plan view of the honeycomb pattern is identical to that of the Large Binocular Telescope (LBT) mirrors and Giant Magellan Telescope (GMT) segments.

4. MANUFACTURING PLAN

Fabrication of the mirror segments follows the same general process used for the MMT, Magellan, LBT, and GMT primary mirrors.[2]-[4] Spin-casting creates the honeycomb sandwich structure and produces a parabolic surface matching M1 to an accuracy of a few mm. We diamond generate, or machine, the mirror to define all critical external surfaces and bring the optical surfaces to an accuracy of about 10 microns rms. We then use actively stressed laps and passive laps for loose-abrasive grinding and polishing of the optical surfaces. We use full-aperture interferometric measurements to guide the figuring and verify that the figure specification is met.

The LSST combined mirror requires several significant modifications to the usual process:

1. The mold for the honeycomb sandwich mirror is made to produce the two optical surfaces, intersecting at r = 2.533 m.
2. The cast mirror blank contains an excess 224 mm of glass over the tertiary mirror, requiring modification of the mold support system, re-evaluation of the annealing and cooling process, and additional machining of glass.
3. We will generate, polish and figure two mirror surfaces on the same blank in the same time frame.

4. Two optical test systems are needed, and the M3 test must be deployable in order to avoid obscuration of the M1 test.
5. We will measure and control the alignment of two optical surfaces.

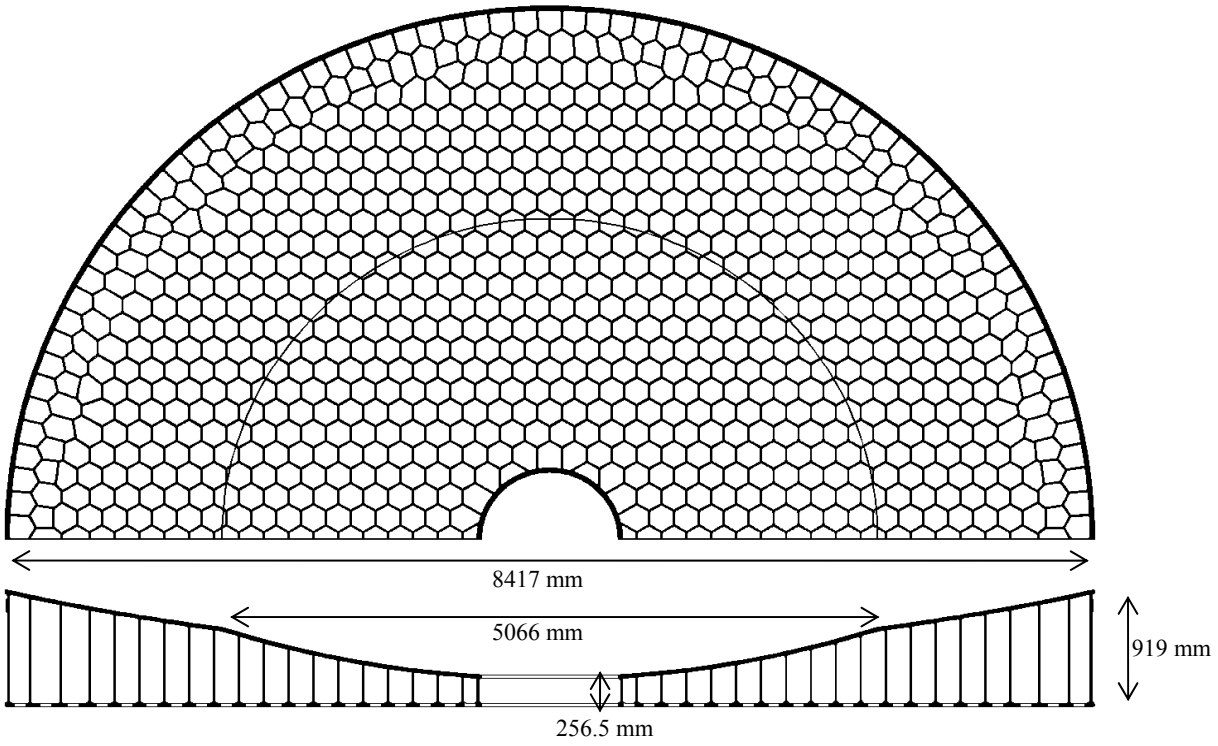

Figure 3. Plan view and cross section of the LSST M1 and M3

5. SPIN-CASTING OF THE COMBINED MIRROR BLANK

5.1 Special considerations for the combined mirror

The LSST combined mirror is the fourth 8.4 m mirror cast at the Mirror Lab, following the two LBT mirrors and the first GMT segment. The extra glass over the LSST tertiary mirror has two potential impacts on the casting process: an increase in mechanical stress due to the mass of glass, and an increase in thermal stress due to the increased glass thickness. We apply a conservative limit of 2.1 MPa (300 psi) maximum tensile stress for stresses applied for more than 5 minutes. As a general rule, we allow 100 psi for annealing stress (due to temperature gradients during anneal, causing stress after the mirror becomes isothermal), 100 psi for temperature gradients, and 100 psi for applied mechanical loads. We modeled the LSST mirror blank through the casting process to determine the stress distribution at all times.

Mechanical stresses would be low if we could maintain a continuous uniform support across the bottom of the mirror throughout the casting. This is not possible because the floor of the furnace bends due to temperature gradients. Once the glass has hardened and annealed, it must be isolated from the bending of the mold. This is achieved by adding counterweight supports that take about 2/3 of the weight of the mirror after annealing. There are constraints on the number and locations of counterweight supports because of interference with the turntable bearing and other components. For the LSST casting we used 72 counterweight supports. Analysis showed that the mechanical stress would be 130 psi because of the increased mass of glass near the center. To compensate for the increased mechanical stress, we set a cooling rate after annealing that would keep thermal stresses below the budgeted 100 psi. The model showed that the maximum thermal stresses did not occur at the same locations as the maximum mechanical stresses, so

we did not have to change the cooling rate significantly. Furthermore, the maximum thermal stresses occur in the primary, not the tertiary, so the extra glass on the tertiary has little impact on the cooling rate. The cooling rate was set to 2.4 K/day during annealing (530-450°C), and 6.7 K/day after annealing. The duration of the casting, from the start of heating until the blank has cooled to room temperature, is 109 days.

5.2 Casting process

Following the standard procedure for honeycomb sandwich mirrors, we built the mold for the LSST mirror blank. The mold consists of a tub of silicon carbide cement and floor tiles, lined with ceramic fiber, and about 1700 hexagonal ceramic fiber boxes to form the cavities in the honeycomb. The tub is held together by inconel steel bands whose tension is maintained by pneumatic cylinders. The glass comes in contact only with the ceramic fiber, which has low strength and little chemical interaction with the glass, and therefore can be separated from the finished mirror blank without applying high stress to the glass. We loaded Ohara E6 borosilicate glass onto the mold in March 2008, and enclosed the mold in the furnace. Heating commenced and the mirror reached its peak temperature of 1165°C on March 29. As of May 26, the mirror has completed the anneal and has cooled to 350°C.

6. GRINDING AND POLISHING

6.1 Generating the two surfaces

We will generate the two optical surfaces with an 8.4 m computer-controlled mill. The mirror rotates on a turntable while the tool follows the desired profile. We use a sequence of three diamond wheels, finishing with a 120 mesh resin-bond wheel with a spherical cutting surface. We normally remove about 10 mm of excess glass, a volume of 0.5 m^3 over an 8.4 m mirror, at a rate of 0.01 m^3/hr with the coarsest wheel. We will generate an additional 2.3 m^3 from the surface of the tertiary mirror, increasing the generating time by about 230 hours or roughly a month.

With the fine wheel, we achieve an accuracy of about 10 microns rms surface, almost all of the error being axisymmetric. We will control mirror thickness and wedge (tilt of the M1 surface relative to the back plate) by caliper measurements at the outer edge. We will control tilt of M3 relative to M1 by measuring axial runout with an indicator.

6.2 Loose-abrasive grinding and polishing

We will lap and polish the mirror surfaces with an 8.4 m computer-controlled polishing machine shown in Figure 4. It has two carriages with horizontal and vertical motion, tool rotation, and rotation of the tool axis to keep it normal to the mirror surface. We use a variety of tools, including actively stressed laps of 1.2 m and 0.3 m diameter and smaller passive laps used with an orbital polishing motion. Each carriage can carry any of these tools.

Most of the figuring is done with stressed laps, which are designed to make the polishing of a highly aspheric surface similar to polishing a sphere. The lap's aluminum plate is bent elastically by computer-controlled actuators to follow the changing curvature of the aspheric surface. The tool can therefore be large and stiff, with a strong smoothing action. The lap is faced with pitch and, for loose-abrasive grinding, a layer of ceramic tiles. To correct figure errors on small scales, we also use an orbital polisher with compliant passive tools of 10 to 40 cm diameter.

To correct axisymmetric figure errors, we vary the lap's rotation rate and horizontal speed as a function of its horizontal position. We have several methods of correcting non-axisymmetric figure errors:

1. Vary the polishing pressure dynamically as a function of mirror rotation angle (increasing removal rate over high regions).
2. Vary the mirror rotation rate dynamically as a function of mirror rotation angle (increasing dwell time over high regions).
3. Have the mirror rotation oscillate between fixed angles (polishing exclusively on high regions).

The first method is used only with the stressed lap, while the other two methods can be used with the stressed lap or the orbital polisher. Axisymmetric figuring and method (1) above allow simultaneous polishing of M1 and M3, using one of the machine's carriages for each surface. Methods (2) and (3) require separate polishing runs on the two surfaces.

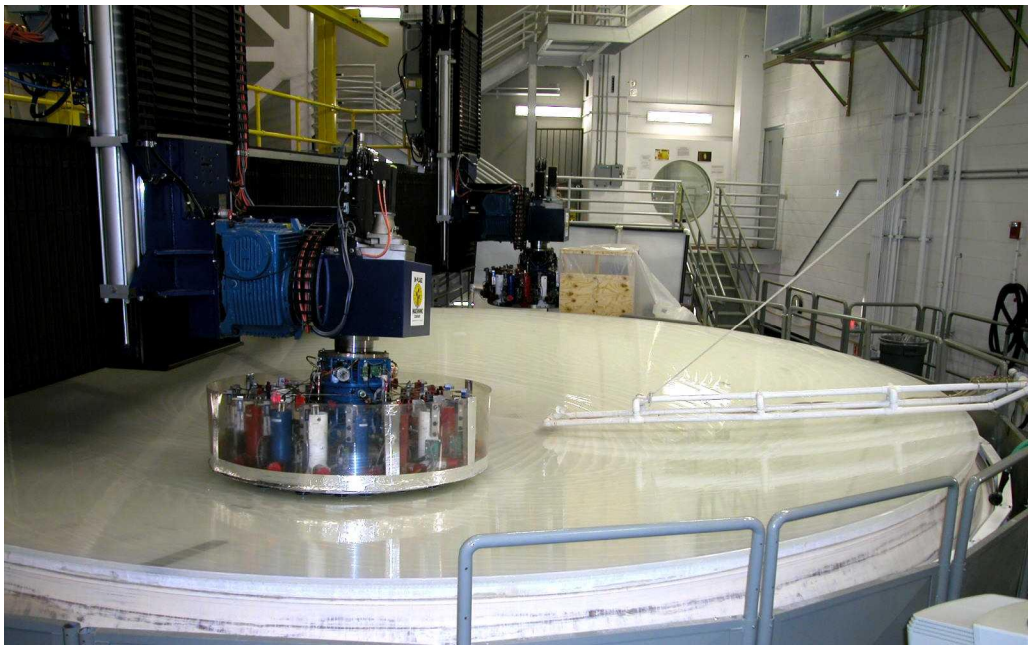

Figure 4. The Mirror Lab's 8.4 m capacity Large Polishing Machine, shown with the second LBT primary mirror. With two carriages, the machine can be used with a variety of actively stressed laps and passive tools. The photo shows two 1.2 m stressed laps.

7. MEASUREMENT

Our philosophy is to measure all critical parameters with two independent methods. For the LSST mirrors, critical parameters include surface figure, radius of curvature, conic constant, and alignment of the two optical axes. We rely heavily on computer-generated holograms for these measurements. Holograms can be written on glass substrates to diffract light with wavefront accuracy well within the LSST tolerances.[5],[6] They also provide convenient mechanical references to the wavefront that enable accurate measurement of alignment parameters and radius of curvature.

We also rely on laser trackers for dimensional and alignment measurements. A laser tracker combines a distance-measuring interferometer with angular encoders to measure displacements of a retroreflector in three dimensions. In addition to the interferometric differential mode, the tracker has an absolute-distance mode that is accurate to roughly 5 parts per million. Angles are measured to better than 1 arcsecond. For most applications, the retroreflector is mounted in a steel ball (sphere-mounted retroreflector, or SMR) and the tracker measures the distance and direction to the vertex of the retroreflector. It can also use a flat mirror as a target, and the direction measured is the normal to the mirror surface.

7.1 Test tower

The Mirror Lab recently completed construction of a 28 m test tower that will support the measurements of the LSST mirrors, GMT segments, and other large mirrors. The new tower, shown in Figure 5, is taller, wider, stiffer and more versatile than the original 24 m tower that was used to measure the MMT, Magellan and LBT primary mirrors. The steel structure is rigidly attached to a triangular concrete plate that is 14 m on a side with ribs 3 m deep. The entire structure rests on pneumatic isolators. Mirrors are moved from the polishing machines to the test tower on an air bearing cart, making the transition a safe and convenient operation.

The tower contains five platforms for access to the test locations of mirrors with a wide range of focal lengths. The test optics for the LSST mirrors will be mounted on carriages that roll on rails to the center of the tower, directly above the mirrors. When the M3 test is in place, its carriage causes a modest obscuration of M1 that has little impact on measurement of low-order aberrations. The M3 test will be moved out of the way to obtain the most complete and accurate measurements of M1's figure.

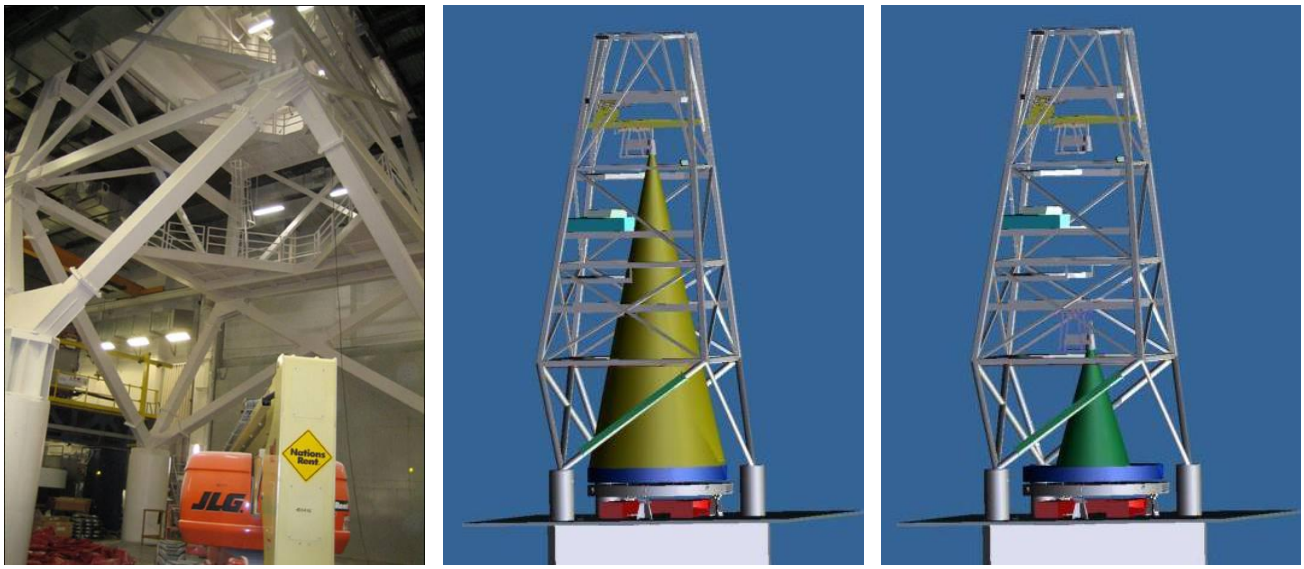

Figure 5. Optical test tower at the Mirror Lab. Models show the configurations for the optical tests of the LSST M1 and M3.

7.2 Figure measurement

We use a vibration-insensitive interferometer to measure the figure of each mirror with a resolution of 20 mm or better on the mirror surface. The test of M1 uses a two-element refractive null lens to compensate for the mirror's aspheric departure. We will use a single diffractive null corrector for the test of M3. The test configurations are shown in Figure 6. We will verify the accuracy of both null correctors by inserting an independent hologram that mimics a perfect mirror surface.[5] When we measure this validation hologram, we expect to see a null wavefront. If we were to see a wavefront error that exceeds the tolerances, it would indicate a mistake in either the null corrector or the validation hologram, and we would have to resolve the discrepancy.

The diffractive null corrector for M3 will be a phase-etched hologram written on a 150 mm diameter flat fused silica substrate. We have used such holographic null correctors for both axisymmetric aspheres and non-symmetric surfaces with modest aspheric departure. (The aspheric departure of M1 is too large to be compensated with a single holographic null corrector.) The hologram for M3 requires rings with spacing as small as 20 μm, which fits well within current production capabilities. The alignment of the hologram to the interferometer is readily performed using an auxiliary hologram that is written on the same substrate. The hologram design is specifically optimized to allow direct measurement and compensation of its substrate errors.[6] The accuracy of the M3 measurement will then be limited to a few nm by the interferometer itself.

7.3 Alignment of the two mirrors

The axial spacings and tilts of both mirrors will be fixed during the generating process and will not change significantly during further processing. All spacings and tilts can be measured easily within the tolerances with a combination of calipers and indicators. The challenging measurements are the lateral displacements. We have two independent methods of measuring the lateral displacements to the 1 mm tolerance.

The first method is the one we have used for all large mirrors, and consists of rotating the mirror by 180° about its mechanical axis and measuring the change in coma. For LSST, this will be done separately for each mirror. The test optics are not moved between the two measurements (0° and 180°). The mirror is tilted to align to the test optics at each position, and the displacement of its mechanical axis (defined by the outer diameter) is measured and controlled.

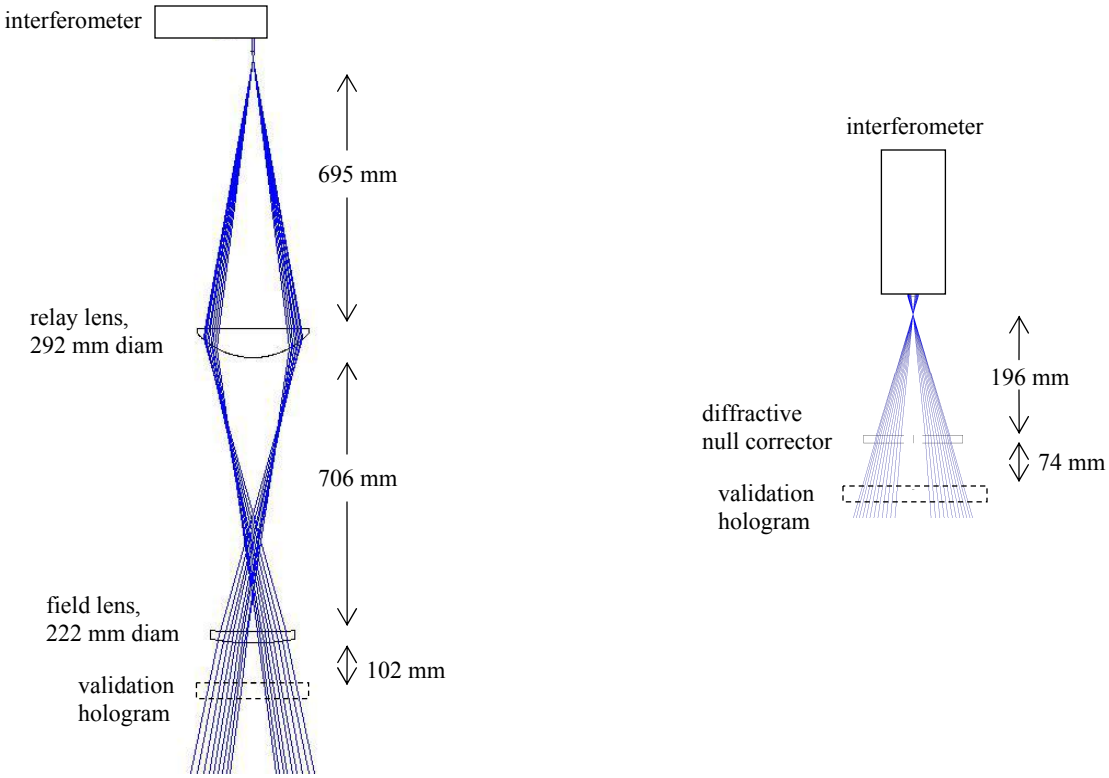

Figure 6. Optical test configurations for the LSST figure measurements, with preliminary dimensions. Each test uses a vibration-insensitive interferometer. We use a two-element refractive null corrector for M1 (left) and a diffractive null corrector for M3 (right). For each null corrector, a validation hologram that mimics the mirror under test can be inserted to verify the accuracy of the null corrector.

A displacement of the mirror's optical axis causes shear of the spherical aberration terms, resulting in coma. A 1 mm lateral displacement causes third-order coma of 580 nm rms surface in M1 and 300 nm rms in M3. We can measure coma to better than 30 nm rms, so the wavefront measurement contributes less than 0.1 mm uncertainty to each mirror's displacement. (We can improve the accuracy further by fitting a model displacement to several measured orders of coma.) We can measure the mirror's physical position to better than 0.2 mm with a laser tracker. Lack of stability in the interferometers' positions and the shapes of the mirrors during the process also contribute errors, but these are minimized by measuring with rotation angles of 0°, 180° and 0° again. We expect to determine the optical axis of each mirror relative to the mechanical axis to better than 0.5 mm. The displacement of M3 relative to M1 will be known to better than 1 mm.

For the second method, the holograms that are used in the test optics for both mirrors serve as alignment references. For M3, we can use either the holographic null corrector or the validation hologram. For M1, we will use the validation hologram. When the test optics are aligned to the mirror surfaces, these holograms define the optical axes to high accuracy. We will measure the position and orientation of each hologram, and the position of the mirror's mechanical axis, with a laser tracker mounted in the center hole of M3. Figure 7 illustrates the method. We use similar methods to align the principal optical test of the GMT.[7] The LSST alignment measurements are simpler and less demanding than the GMT measurements.

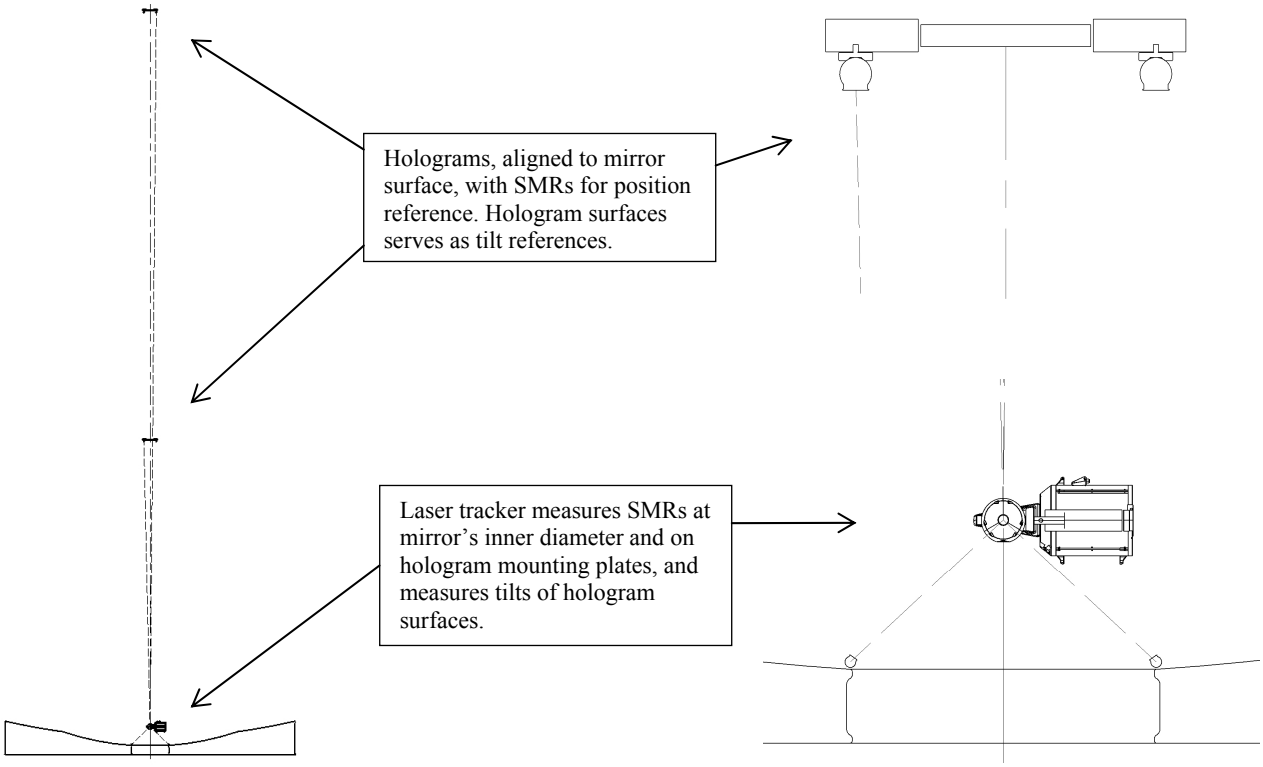

Figure 7. Illustration of the measurement of lateral displacements of the mirrors' optical axes, using the holograms as references

For the LSST alignment measurements, we will mount SMRs on the hologram's mounting plate and measure their positions relative to the hologram pattern with an optical coordinate-measuring machine (CMM) in the lab. When the hologram is aligned to the mirror, we will measure the positions of these SMRs with the laser tracker, and measure the tilt of the hologram through a reflection off the lower surface of the hologram substrate. (The hologram for M1 will be visible only when the test optics for M3 are moved out of the way.) We will also determine the mechanical center of the combined mirror by measuring SMRs at the inner diameter of M3. The measurement sequence is as follows:

1. Align M1 to its optical test and measure the wavefront.
2. Insert the M1 validation hologram, align it to the test optics, and measure the wavefront.
3. Deploy the M3 test system, align it to the mirror, and measure the wavefront.
4. Measure the SMRs at the inner edge of M3 with the laser tracker.
5. Measure the position and orientation of the M3 hologram with the laser tracker.
6. Remove the M3 test system.
7. Measure the position and orientation of the M1 hologram with the laser tracker.

The wavefront measurements will be repeated as necessary to verify the stability of the system.

The result of this sequence is measurement of the optical axes of both mirrors and the mechanical center of the primary mirror. Table 3 gives a conservative estimate of the accuracy of measurement. The hologram is aligned to the mirror by measuring coma for both wavefronts (hologram and mirror); an uncertainty of 60 nm rms surface is assumed. The positions of the SMRs relative to the holograms will be measured with an optical CMM, and the SMRs at the inner edge of the mirror will be fixed relative to the inner diameter and the mirror surface by a kinematic mount. The laser tracker's measurement of the SMRs on the hologram mounts is limited by the tracker's angular accuracy, assumed to be 2 arcseconds. We also assume a 2 arcsecond accuracy for the tracker measurement of tilt of both holograms. This uncertainty in tilt is projected from the hologram to the mirror to give the displacements listed in the table. The net

uncertainty in displacement of each mirror's optical axis at the mirror surface is 0.3 mm in *x* and *y*, while the uncertainty in the mechanical center is 0.2 mm in *x* and *y*. These uncertainties yield a net uncertainty of 0.4 mm in *x* and *y* for the primary mirror relative to the mechanical center and for the tertiary relative to the primary. Combining uncertainties in *x* and *y*, we will know the relative positions of the axes to better than 0.6 mm.

Table 3. Estimated measurement accuracy for lateral displacement of the optical axes, using the holograms as alignment references. The displacements apply to one axis, *x* or *y*. Units are mm.

source	M1	M3	mechanical center
alignment of hologram to mirror	0.1	0.2	
position of SMRs relative to axis	0.1	0.1	0.2
measurement of SMR positions	0.2	0.1	0.1
measurement of axis tilt	0.2	0.1	
sum in quadrature	0.3	0.3	0.2

We expect to see agreement between the two independent methods of measuring the alignment of the optical axes. If we find either axis to be out of its tolerance, this is equivalent to coma in the mirror surface. We will add the coma terms to the figure measurements and polish them out using the techniques described in Section 6.2. We can correct either or both surfaces to bring the axes into alignment. We would generally choose the correction that minimizes the removal of glass.

7.4 Radius of curvature and conic constant

We have traditionally measured the radius of curvature of large mirrors with a calibrated steel tape. The validation hologram serves as a mechanical reference for the mirror's center of curvature. The interferometer and null corrector are first aligned to the mirror, then the validation hologram is inserted and aligned to the test optics. We use the tape to measure the distance from the hologram to a bar spanning the center hole of the mirror. Adjustments are made for the thicknesses of various mechanical fixtures, thermal and elastic expansion of the tape, sag of the bar, and power in the wavefront of the mirror and the hologram. The measurement can be made to an accuracy of 0.5 mm for M1 and better for M3.

For the LSST mirrors we will also measure the radii with a laser tracker. Again, the holograms will serve as mechanical references to the centers of curvature. This measurement comes almost for free as part of the alignment measurement illustrated in Figure 7. To measure the radius of M1, it is necessary to mount SMRs on the surface of M1, in addition to those mounted at the inner edge of the M3 surface as shown in the figure. We expect this measurement to be more accurate than the steel tape.

The conic constant is determined independently by the null corrector and the validation hologram. An error in conic constant is equivalent to spherical aberration in the wavefront. The null correctors are designed to convert a spherical wavefront into the correct asphere with the right amount of spherical aberration. Each validation hologram is designed by propagating the surface of a perfect mirror up to its paraxial center of curvature and taking a planar slice across the wavefront. Its design is independent of the corresponding null corrector.

One measure of conic constant comes directly from the measurement of the mirror with the null corrector. Our tolerance analysis indicates that it will be accurate to about 100 parts per million (ppm) for M1 and 50 ppm for M3. The second measurement comes from using the validation hologram to calibrate the null corrector, treating the validation hologram as the standard and using the null corrector to compare the mirror figure against that standard. The validation holograms are expected to be accurate to 50 ppm in conic constant.

8. SUMMARY

We have described a manufacturing plan for the LSST combined mirror that will comfortably meet the accuracy requirements. We have designed redundant measurements of all critical parameters, including mirror figure, radius of curvature, conic constant, and alignment of the optical axes. The measurements make use of computer-generated holograms for wavefront compensation and as alignment references.

The honeycomb sandwich blank for the combined mirror has been cast and is cooling toward room temperature. Through the production of a number of 6.5 m and 8.4 m honeycomb mirrors, we have developed efficient methods of fabrication and are ready to apply them to the LSST mirror surfaces.

REFERENCES

[1] D. W. Sweeney, "Overview of the Large Synoptic Survey Telescope project", in *Ground-based and Airborne Telescopes*, ed. L. M. Stepp, Proc. SPIE 6267 (2006).

[2] B. H. Olbert, J. R. P. Angel, J. M. Hill and S. F. Hinman, "Casting 6.5-meter mirrors for the MMT conversion and Magellan", in *Advanced Technology Optical Telescopes V*, ed. L. M. Stepp, Proc. SPIE 2199, p. 144 (1994).

[3] H. M. Martin, R. G. Allen, J. H. Burge, L. R. Dettmann, D. A. Ketelsen, S. M. Miller and J. M. Sasian, "Fabrication of mirrors for the Magellan Telescopes and the Large Binocular Telescope", in *Large Ground-based Telescopes*, ed. J. M. Oschmann and L. M. Stepp, Proc. SPIE 4837, p. 609 (2003).

[4] H. M. Martin, R. G. Allen, B. Cuerden, J. M. Hill, D. A. Ketelsen, S. M. Miller, J. M. Sasian, M. T. Tuell and S. Warner, "Manufacture of the second 8.4 m primary mirror for the Large Binocular Telescope", in *Optomechanical Technologies for Astronomy*, ed. E. Atad-Ettedgui, J. Antebi and D. Lemke, Proc. SPIE 6273 (2006).

[5] J. H. Burge, "Certification of null correctors for primary mirrors", in *Advanced Optical Manufacturing and Testing IV*, J. Doherty, Editor, Proc. SPIE 1994, 248-259 (1993).

[6] P. Zhou and J. H. Burge, "Optimal design of computer-generated holograms to minimize sensitivity to fabrication errors", Opt. Express **15**, 15410-15417 (2007).

[7] J. H. Burge, W. Davison, C. Zhao and H. M. Martin, "Development of surface metrology for the Giant Magellan Telescope primary mirror", in *Advanced Optical and Mechanical Technologies in Telescopes and Instrumentation*, ed. E. Atad-Ettedgui and D. Lemke, Proc. SPIE 7018 (2008).